Food web constraints on larval growth in subtropical coral reef and pelagic fishes

Miram R. Gleiber[1],*, Su Sponaugle[1], Kelly L. Robinson[2], Robert K. Cowen[3]

[1]Department of Integrative Biology, Hatfield Marine Science Center, Oregon State University, Newport, Oregon 97365, USA
[2]Department of Biology, University of Louisiana at Lafayette, Lafayette, Louisiana 70503, USA
[3]Hatfield Marine Science Center, Oregon State University, Newport, Oregon 97365, USA

ABSTRACT: Prey availability and predation pressure are thought to be key constraints on larval growth, especially in low-productivity, subtropical environments. Yet, measuring their effects on larval fishes has been challenging, given the dynamic biophysical drivers of plankton distributions and small scales of interactions. We integrated fine-scale net tows (10s of meters) with *in situ* imaging to explore how predator–prey interactions influence larval fish growth in the Straits of Florida. Otolith-derived recent growth was analyzed for 3 ecologically important fishes: 2 coral reef labrids (*Thalassoma bifasciatum* and *Xyrichtys novacula*) and 1 tuna (*Katsuwonus pelamis*), with differing mean growth rates (labrids 0.25 mm d^{-1}, *K. pelamis* 0.44 mm d^{-1}) and prey (labrids–copepods; tuna–appendicularians). We used generalized additive models to examine the interactive effect of background density and frequency of elevated (>2 SD above background) prey and predators on recent (last 3 d) larval growth. For all taxa, recent growth increased with prey background density. Recent growth of labrids was also higher when copepod densities were more often elevated (14% of transect >20 ind. m^{-3}) above otherwise low background densities (2 ind. m^{-3}). Predators (chaetognaths and hydromedusae) had a growth-selective effect: stronger selection in transects with high-density predator patches, although the direction of the effect was species-specific. The effect of temperature was taxa-specific: growth increased with temperature for the labrids and peaked at an optimum (28°C) for the rapidly growing tuna. Integration of these fine-scale sampling methods improves our understanding of the variable influence of prey and predators on larval growth and, consequently, larval survival.

KEY WORDS: Larval fish · Growth · Patchiness · Prey · Predators · Fine-scale · Tuna · Wrasse

1. INTRODUCTION

The pelagic larval phase of most marine fishes is characterized by high mortality rates that influence patterns of recruitment and subsequent adult population dynamics (Hjort 1914). Larval survival and growth during this phase (weeks to months) depends on the ability of larvae to find food and avoid predation (Houde 1987). Their success doing so often impacts cohort strength (Ringuette et al. 2002, Castonguay et al. 2008). Studies have suggested that patches of dense aggregations of prey, as opposed to average densities, are key to larval survival due to increased larva-prey encounter rates that optimize foraging in an often prey-limited pelagic environment (Lasker 1975, Houde 1987, Rothschild & Osborn 1988).

Prey and predator aggregations, from fine (meters) to large scales (kilometers), occur along biological gradients formed by physical processes such as fronts, eddies, stratification, and upwelling (Mackas et al. 1985, Owen 1989, Richardson et al. 2009, Greer et al. 2013). While decades of research points to the critical role of patchiness of planktonic prey to larval fishes (Mackenzie et al. 1990, Davis et al. 1991, Young et al. 2009), we lack empirical studies examining relation-

ships between prey patchiness and larval fish growth and survival. Furthermore, understanding the direct effects of predator distributions on larval fishes has been difficult, if not impossible, given the small scale of the interactions and dynamic biophysical drivers of predator and prey distributions (Greer et al. 2013). Traditional net sampling has previously limited the scale over which these questions can be asked (but see Bils et al. 2017), as integrating prey over large spatial scales obscures relationships between prey availability, larval feeding success, and predation pressure (Pepin 2004, Young et al. 2009). However, advances in sampling technology now allow us to use *in situ* measurements (high-resolution imaging) to look beyond 'average' scenarios to examine consequences of spatial variability in zoo- and ichthyo-plankton aggregations for trophic interactions (Greer et al. 2013, 2016, Greer & Woodson 2016).

Larval fish growth is a valuable tool for understanding how variability in the prey (or predator) environment relates to success. Growth is recorded via the daily deposition of concentric increments in fish otoliths (ear stones) in proportion to their somatic growth, with wider increments indicating faster growth (Pannella 1971). High larval growth rates increase the probability of survival by reducing vulnerability to gape-limited predation and duration of larval stage (Miller et al. 1988, Houde 1989, Hare & Cowen 1997) but can also influence juvenile survivorship by determining condition at metamorphosis/settlement (Searcy & Sponaugle 2001, Hamilton 2008). Larval growth has been consistently linked to feeding success across taxa and environments (Dower et al. 2009, Sponaugle et al. 2009, Pepin et al. 2014), but few studies have examined how larval growth is directly related to prey availability (Wexler et al. 2007, Satoh et al. 2013). Over larger scales, productive oceanographic physical features (e.g. fronts, mesoscale eddies) have been shown to enhance larval growth (Shulzitski et al. 2015), condition (Nakata et al. 2000), and survival to settlement (Shulzitski et al. 2016), likely due to increased prey availability. Additionally, studies on individual larvae have demonstrated that variability in feeding and growth rates due to stochastic feeding events play a key role in larval success within cohorts (Pepin 2004, Dower et al. 2009, Pepin et al. 2014, Robert et al. 2014), suggesting prey patchiness as an essential component of larval growth and survival. However, the examination of larval growth with regard to variation in natural prey patchiness has not been possible.

In addition to the importance of prey availability for larval fishes, predator densities have the poten-tial to influence larval survivorship. Mortality is often selective, with predators removing smaller, slower-growing individuals from the population (Anderson 1988, Bailey & Houde 1989, Hare & Cowen 1997, Takasuka et al. 2003), although the opposite direction of selective mortality has been also documented (Sponaugle et al. 2011, Takasuka et al. 2017). Non-random predation can obscure the effect of variable prey conditions on larval growth (Meekan & Fortier 1996, Robert et al. 2007), so quantifying this effect is important. While it is difficult to study the direct role of predation on larval fishes in nature, the selective influence of predators can be inferred through the examination of otolith-based growth trends in a larval population. For example, predator removal of small or slow growers increases the apparent average growth and size-at-age of a sampled population (survivors). High-density patches of predators have the potential to exert a strong selective pressure on a larval fish population, but fine-scale examination of larval growth trends and corresponding predator and prey densities are required to tease apart the influence of predators and prey on larval growth.

We used coupled fine-scale *in situ* imaging with biological sampling to examine how local prey and predator densities and patchiness influence larval fish growth for 2 coral reef fishes and 1 tuna in the Straits of Florida (SOF). The SOF is a region characterized by a high abundance and diversity of larval fishes imbedded within a fast-flowing major western boundary current. Regional physical processes (cyclonic mesoscale eddies and upwelling) that elevate prey concentrations translate to higher gut fullness and growth in larval fishes on broad scales (Sponaugle et al. 2009, Llopiz et al. 2010, Shulzitski et al. 2015). Assuming high density prey patches similarly influence larval traits on fine scales, we expected high prey availability in frequent patches (reduced prey search time) to enhance growth. While our understanding of the effect of predator densities on larval growth is limited, modeling studies suggest high predation pressure, such as high-density patches of predators, is needed to see evidence of size-selective losses (Paradis et al. 1999). Studies of selective mortality on coral reef larvae in the SOF have shown selection against both slow-growing (Shulzitski et al. 2016) and fast-growing larvae (Sponaugle et al. 2011). Therefore, it is difficult to predict the direction of selective loss, but we hypothesized that the strength of selective mortality (regardless of direction) will increase with high densities, and more frequent patches, of predators.

2. MATERIALS AND METHODS

2.1. Study area

The SOF is bordered by the Florida Keys to the west and the Bahamas to the east (Fig. 1). Flow through the SOF is dominated by the rapid Florida Current (average speed: 160 cm s^{-1}; Lee et al. 1991), which links the Gulf of Mexico and Caribbean to the Gulf Stream in the North Atlantic. The Florida Current is stronger and more dynamic along the northwest/west (Florida Keys) side of the SOF and generates cyclonic mesoscale and sub-mesoscale eddies in addition to western boundary current upwelling (Hitchcock et al. 2005). These physical processes result in cross-strait variability in nutrients, primary productivity, zooplankton, and larval fishes, with generally higher values in western waters compared to the eastern SOF (Lee et al. 1991, Richardson et al. 2010, Shulzitski et al. 2018).

2.2. Field sampling

To examine otolith-derived growth in larval fishes and fine-scale distributions of their prey and predators, we collected biological samples together with *in situ* plankton imagery. Sampling was conducted on 2 cruises in the SOF aboard the R/V 'FG Walton Smith' from 28 May to 6 June 2014 and 18 to 26 June 2015. Each year, we sampled 8 stations encompassing the north-south and cross-strait variability in the SOF (Fig. 1). At each station, we used the *in situ* ichthyoplankton imaging system (*IS*IIS; Cowen & Guigand 2008) to measure zooplankton distributions. We sampled the water column at each station with two 8 to 16 km transects sampling at discrete depths of 15 and 30 m (Fig. 1). Towed at a speed of 2.5 m s^{-1}, the *IS*IIS imaged the water column at ~140 l s^{-1} with a pixel resolution of 55 to 68 μm, imaging particles from ~200 μm to 13 cm. Sensors on *IS*IIS simultaneously measured conductivity, temperature, and depth.

Larval fishes were collected at each station using a multiple opening/closing net and environmental sensing system (MOCNESS) with a 4 m^2 opening and 1 mm mesh nets. The MOCNESS is equipped with sensors that simultaneously measured conductivity, temperature, and depth. To capture larval fishes and mesozooplankton on a fine horizontal spatial scale, we sequentially fired each MOCNESS net
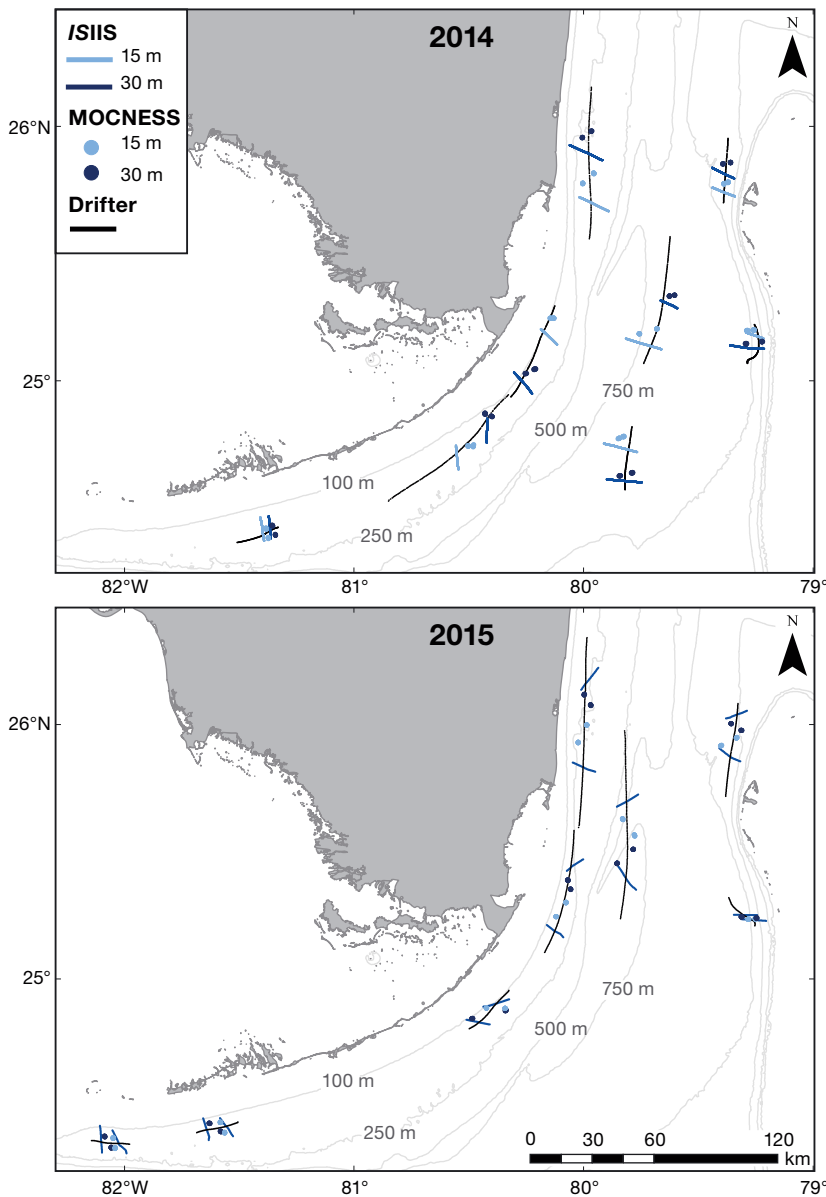

Fig. 1. Locations in the Straits of Florida (SOF) sampled in (top) May to June 2014 and (bottom) June 2015. Multiple opening/closing net and environmental sensing system (MOCNESS) replicate tows and *in situ* ichthyoplankton imaging system (*IS*IIS) transects at each depth (15 and 30 m) were centered on a drogue that drifted northeastward with the Florida Current. Distances between MOCNESS tows and *IS*IIS transects appear farther apart in the western SOF where the Florida Current is stronger, compared to east SOF, but in all regions the same water mass was sampled in a moving current. Map generated using ArcGIS v.10.6 (www.esri.com)

every ~125 m. Traveling at a speed of 1 m s^{-1}, each MOCNESS net sampled ~500 m^3. We fired a total of 5 nets per tow: 1 net was open from the surface to depth (net zero; not included in analysis), and the 4 remaining nets sampled sequentially at the same depth, either 15 or 30 m. At every station, this fine-scale net sampling was repeated with 2 complete MOCNESS tows (depth determined in randomized order), yielding 8 replicate nets per depth (Fig. 1). Once onboard, the nets were rinsed with seawater and the contents of each cod end preserved in 95% ethanol. To reduce degradation of otoliths, ethanol was changed after 24 to 48 h and again after 2 to 3 mo for high biomass samples. All larval fishes were separated out of the samples in the laboratory and identified to the lowest possible taxonomic grouping following Richards (2005).

To ensure all *IS*IIS and MOCNESS transects sampled the same water mass, transects and tows at each depth were centered on a GPS Lagrangian drifter at 10 m depth, moving with the Florida Current (Fig. 1). Each replicate MOCNESS tow (4 nets) per depth at each station corresponded with one half of the *IS*IIS transects (half-transects = 4 to 8 km). All sampling occurred during daylight hours, approximately 06:00−18:00 h, to minimize diel effects and because larval fish typically feed during daylight hours in the SOF (Llopiz & Cowen 2009, Llopiz et al. 2010).

2.3. Otolith analysis

We used otolith microstructure analysis to obtain data on larval age and daily growth (increment widths) for individual larvae. Based on sample size, confirmation of daily increment deposition (Victor 1982, Radtke 1983, Hare & Cowen 1991, Tanabe et al. 2003) and our ability to morphologically identify larvae to species, 2 coral reef wrasses and 1 tuna were selected for otolith analyses: bluehead wrasse *Thalassoma bifasciatum*, pearly razorfish *Xyrichtys novacula* and skipjack tuna *Katsuwonus pelamis.* All larvae collected of *T. biasciatum* (n = 339), *X. novacula* (n = 479), and *K. pelamis* (n = 295) were measured for standard length (SL) using a Leica dissecting microscope with camera and image analysis software (Image-Pro Plus 7.0 and Premier 9.3). We analyzed the otolith microstructure on a subset of larvae (n = 6 to 19) from a subset of replicate tows at different stations/depths (n = 14 to 19; depending on availability of each species). The size distribution of the subset of larvae used for otolith analysis (*T. bifasciatum:* n = 147, *X. novacula*: n = 156, *K. pelamis*: n = 134) was proportional to all larvae of that species in each tow (Fig. 2).
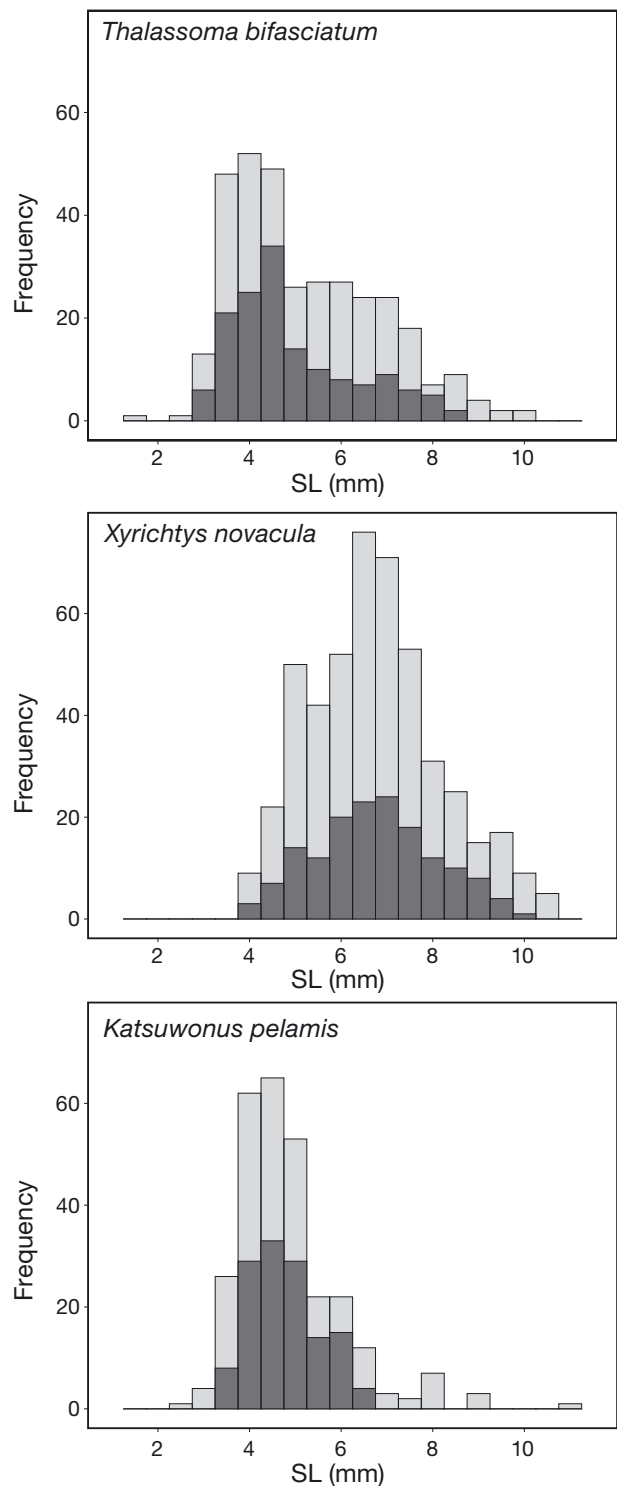

Fig. 2. Size class frequency of larval (a) *Thalassoma bifasciatum*, (b) *Xyrichtys novacula*, and (c) *Katsuwonus pelamis* sampled from all tows (light gray; n = 64 tows) and from larvae selected for otolith analysis (dark gray). Number of larvae in all tows (light gray): 339 (*T. bifasciatum*), 479 (*X. novacula*), 295 (*K. pelamis*). Number of larvae in otolith analyses (dark gray): 147 (*T. bifasciatum*), 156 (*X. novacula*), 134 (*K. pelamis*)

Sagittal otoliths were extracted and stored in immersion oil on a glass slide to facilitate reading (Sponaugle 2009). Prepared otoliths were read along the longest axis at 1000 (oil immersion) magnification using a Leica compound microscope with a camera attachment and Image-Pro Premier 9.3. Otoliths were read 2 to 3 times by the same reader, and if reads did not differ by >5%, 1 read was randomly chosen for analysis. Otoliths where 3 reads all differed by >5% were removed from further analysis (Sponaugle 2009).

2.4. *IS*IIS image analysis

Zooplankton taxa were sorted into image classes based on taxonomy and morphology with an automated algorithm. *IS*IIS raw image files were flatfielded and segmented with methods described by Luo et al. (2018). Segmented images were classified using a Sparse Convolutional Neural Network (Graham 2014), following the methods developed by Luo et al. (2018). The algorithm was implemented with training sets (different for each sampling year) composed of 124 classes representing 40 broader groups (e.g. classes of different shapes or orientations of chaetognaths combined into a single 'Chaetognath' group; Schmid et al. 2020). Automated image classifications were corrected for misclassifications with scaling factors determined by confusion matrices. The confusion matrices were created separately for each year from a random subset of images (0.005% of all ~100 million classified images) that were manually classified (Luo et al. 2018, Schmid et al. 2020).

Physical data and biological counts from image analyses were synchronized using the sample time stamp and quantified by 1 m horizontal distance bins. Corrected counts (see above) of organisms in each classification group were used to estimate plankton densities (ind. m^{-3}) based on the volume of water sampled by *IS*IIS in each 1 m horizontal bin.

2.5. Fine-scale prey/predator availability

Environmental prey/predator availability and fine-scale distributions from *IS*IIS imagery were summarized with 2 variables for comparison with recent larval growth: background density (BD) and frequency elevated (FE). BD was calculated as the mean of the 1 m horizontal bin densities (ind. m^{-3}) in each *IS*IIS half-transect. FE was calculated as the percentage of 1 m horizontal bins in an *IS*IIS half-transect where the density was >2 standard deviations (SD) above

the BD. Prey groups from *IS*IIS considered in this study were determined from previous gut content analyses in the SOF: 'appendicularians' for *K. pelamis* (Llopiz et al. 2010) and 'copepod other' (a morphological classification including copepods without visible antennae) for *T. bifasciatum* and *X. novacula*. The wrasses consume a mixed diet of harpacticoid and cyclopoid (e.g. *Oncaea* sp., *Farranula* sp., but not *Oithona* sp.) copepods (Llopiz & Cowen 2009, Sponaugle et al. 2009), but because *IS*IIS imagery cannot distinguish between some taxa with similar morphologies, these groups were combined in the 'copepod other' group. Predator groups from *IS*IIS included 'chaetognaths' and 'hydromedusae', the most abundant potential predators of larval fishes in the SOF (Bailey & Houde 1989, Purcell & Arai 2001 and references therein; unpubl. data). The 2 predator groups were combined for BD and FE calculations because, separately, chaetognath and hydromedusae densities were strongly correlated (r = 0.88).

2.6. Recent growth analysis

We compared variability in larval growth with prey/predator availability by computing 'recent growth' (as a detrended growth index) for all species from the average of the last 3 complete otolith increment widths. As it is unknown how long the larvae had been associated with the sampled prey/predator conditions (days to weeks), we used recent growth as a proxy for the last 3 full days of growth prior to capture (Sponaugle et al. 2010, Shulzitski et al. 2015). This is also the amount of time for feeding to influence nutritional condition (Clemmesen 1994).

Since increment width and variability increases with age, we detrended the last 3 increment widths by age to allow for the comparison of recent growth of different aged larvae (Baumann et al. 2003). A detrended growth index was computed using:

$$\mathrm{DG}_{ij} = (G_{ij} - G_j)\,\mathrm{SD}_j^{-1} \qquad (1)$$

where DG_{ij} is the detrended growth of individual *i* at age *j*, G_{ij} is otolith growth (increment width) for individual *i* at age *j*, G_j is the mean of otolith growth of all individuals at age *j*, and SD is the standard deviation of *G* (Sponaugle et al. 2010). For each species, we compared detrended recent growth across prey densities, predator densities, temperatures, depths, and years using separate analysis of covariance (ANCOVA) with age as a covariate, to confirm there was not a significant interaction between age and each variable.

2.7. Modeling approach

We examined the effect of local prey and predator availability on recent growth for each larval fish species using generalized additive models (GAMs) with a Gaussian distribution. These non-parametric regression techniques allow for non-linear relationships between dependent and independent covariates (Wood 2006). GAMs are modeled using smoothing functions with additive techniques where all covariates are independent, allowing for easy inference, as the effect of each covariate is the same regardless of the values of the remaining covariates. The model for each species included detrended recent growth from 147 (*T. bifasciatum*), 156 (*X. novacula*), or 134 (*K. pelamis*) larvae and their associated prey/predator BD and FE from *IS*IIS half-transects corresponding to each MOCNESS tow (n = 18, 19, and 14, respectively). Temperature, depth, and otolith-derived early growth (for wrasses) were included as covariates. Since larval fishes can have serial correlation in daily otolith-derived growth (Dower et al. 2009, Pepin et al. 2014, Robert et al. 2014), an early growth variable (average increment width from Days 5 to 10) was included in the model. Early growth was not included for *K. pelamis* since their ages ranged from only 4 to 11 d (mean = 7.1 d); thus, mean recent growth (last 3 full days of life) of the younger larvae included the earliest days of growth. Temperature was from MOCNESS environmental data, averaged across each tow. While larval density can influence growth due to competition for resources, density dependence was not appropriate to consider in the models since larval fishes in the SOF are rare compared to their planktonic prey and predators. In fact, the copepod and appedicularian prey are, on average, ~500 and ~9000 times more abundant than their respective larval fish predators (wrasses and tuna).

We examined the additive and interactive effects of prey or predator BD and FE on recent larval fish growth with 2 model formulations for each species: a GAM and an interactive GAM (Table 1). Fixed covariates were PreyBD (continuous), PreyFE (continuous), PredatorBD (continuous), PredatorFE (continuous), Temperature (continuous), EarlyGrowth (continuous), and Depth (categorical with 2 levels). The interaction terms in the interactive GAM were PreyBD × PreyFE and PredatorBD × PredatorFE. Smoothing functions were applied to continuous variables, and tensor product smoothers were included for interactions as they are more appropriate for interactions fitted to covariates with different units. To avoid model overfitting, the number of knots used in the smoothers and tensor product smoothers were restricted to 4 and 8, respectively. Density variables were log transformed since prey and predator densities each range over an order of magnitude. Prior to the GAM analyses, we used variance inflation factor (VIF) analysis to detect collinear variables and removed those variables above a VIF cut-off of 3. For *K. pelamis*, there was collinearity between prey and predator BD and between predator BD and FE. Therefore, we formulated separate prey and predator models for *K. pelamis* and were unable to include an interactive GAM for predators (Table 1).

Model selection was performed using a backward stepwise approach. Full and reduced versions of the models were compared using Akaike's information criterion (AIC) as a measure of goodness of fit and generalized cross validation (GCV) as a measure of the model's predictive performance. The best model was identified by minimizing both AIC and GCV. We incorporated the dependency of growth on larvae collected from the same MOCNESS tow by including a random intercept in the fixed model, but AIC determined models without a random effect were best.

Table 1. Generalized additive models (GAM) used to examine the influence of prey and predator distributions on recent larval growth patterns of *Thalassoma bifasciatum*, *Xyrichtys novacula*, and *Katsuwonus pelamis* in the Straits of Florida. Due to collinearity, *K. pelamis* has separate prey and predator (background density only) GAMs; a predator interactive GAM could not be performed. *G*: recent growth (mean of last 3 full otolith increment widths as a detrended growth index); PreyBD: prey background density ($\log_{10}$ transformed); PreyFE: prey frequency elevated; PredBD: predator background density ($\log_{10}$ transformed); PredFE: predator frequency elevated; *T*: temperature; EarlyGrowth: mean of otolith increment widths 5–10

GAM formulations	
T. bifasciatum, X. novacula	*G* = PreyBD + PreyFE + PredBD + PredFE + Depth + *T* + EarlyGrowth
K. pelamis (prey)	*G* = PreyBD + PreyFE + Depth + *T*
K. pelamis (predator)	*G* = PredBD + Depth + *T*
Interactive GAM formulations	
T. bifasciatum, X. novacula	*G* = PreyBD × PreyFE + PredBD × PredFE + Depth + *T* + EarlyGrowth
K. pelamis (prey)	*G* = PreyBD × PreyFE + Depth + *T*

Model diagnostics and residuals were checked for potential deviations from normality assumption, homogeneity of variance, and other anomalies. All calculations and models were coded in R software (v.3.6.0; R Core Team 2019) using the *mgcv* library.

3. RESULTS

3.1. Larval fish characteristics

Larval densities of *Thalassoma bifasciatum*, *Xyrichtys. novacula*, and *Katsowonus pelamis* from all tows were 2.94 ± 6.92, 3.89 ± 11.21, and 2.37 ± 3.89 ind. 1000 m^{-3}, respectively (mean $\pm$ SD, n = 64). Mean densities from the subset of replicate tows included in otolith analyses for each species were 8.41 ± 8.58 (n = 18), 10.05 ± 16.71 (n = 19), and 7.39 ± 3.21 ind. 1000 m^{-3} (n = 14). All 3 species had a roughly similar size range (Fig. 2). However, because *K. pelamis* is a rapidly growing species with somatic growth rates of 0.44 mm d^{-1} (linear regression), compared to the wrasses (*T. bifasciatum*: 0.21 mm d^{-1}, *X. novacula*: 0.27 mm d^{-1}), tuna larvae were substantially younger (4–11 d; mean = 7.1 ± 1.4 d) than either wrasse (15–45 d; *T. bifasciatum*: mean = 26.0 ± 6.1 d, *X. novacula*: 25.8 ± 4.1 d). Mean size of *X. novacula* (6.74 ± 1.32 mm SL) tended to be larger than *T. bifasciatum* (4.96 ± 1.36 mm) and *K. pelamis* (4.79 ± 0.76 mm).

3.2. Fine-scale prey/predator availability

The appendicularian prey of *K. pelamis* were more abundant and pervasive compared to the copepod (cyclopoid and harpacticoid) prey of the wrasses (*T. bifasciatum*, *X. novacula*). Appendicularian background densities (BD) ranged from 30 to

111 ind. m^{-3}, 5- to 10-fold greater than the copepod BD ranging from 2 to 20 ind. m^{-3} (Table 2). The copepods had more variability in their fine-scale distribution with frequent high-density patches of prey in some regions, where up to 14% of the transect had elevated densities (FE; Table 2). When copepod prey were elevated, their densities were 3- to 27-fold greater than BD. In contrast, the appendicularians had lower and less variable FE with only 2 to 5% of the transect having elevated densities (Table 2). When elevated, densities were only 2- to 5-fold greater than BD. The BD of the predators (chaetognaths and hydromedusae, combined) ranged from 6 to 73 ind. m^{-3} (Table 2). Predators were pervasive and less variable in distribution, similar to appendicularians, with elevated densities in only 3 to 6% of the transect. When elevated, densities were 2- to 19-fold greater than BD.

3.3. Modeled relative recent growth

Both the GAMs and interactive GAMs revealed clear influences of prey, predators, and temperature on larval fish recent growth. For all species, both types of models performed similarly, but we focus primarily on the interactive GAMs (Figs. 3 & 4) since they provide additional insights on the multiplicative effect of BD and FE of prey and predators. However, we had to focus on GAM results for *K. pelamis* (predator model) since an interactive GAM was unable to be performed due to collinearity between predator BD and FE (Fig. 4c,d). GAM results are provided for other species in the Supplement to illustrate the more simple, univariate responses (Figs. S1–S3 at www.int-res.com/articles/suppl/m650p019_supp.pdf).

Recent growth of *T. bifasciatum* significantly increased across gradients of both prey (copepods) BD

Table 2. Summary of background densities (BD) and frequency elevated (FE) of prey and predator groups from *IS*IIS transects associated with larval fish growth data from the Straits of Florida. BD is the average density of 1 m horizontal bin densities (ind. m^{-3}) in each *IS*IIS half-transect. FE is the percentage of 1 m horizontal bins in an *IS*IIS half-transect where the density is >2 standard deviations (SD) above the BD. Number of *IS*IIS half-transects = 30 (copepods), 14 (appendicularians), 34 (predators). Elevated density minimum is the density threshold for 1 m horizontal *IS*IIS bins to be considered elevated: mean BD + 2 SD of 1 m bins in each transect. Elevated density is the density of 1 m horizontal bins above the elevated density minimum; 1 m bins included in FE. Number of 1 m bins per transect = 3341 to 11217 (mean = 6272). Data are mean (range)

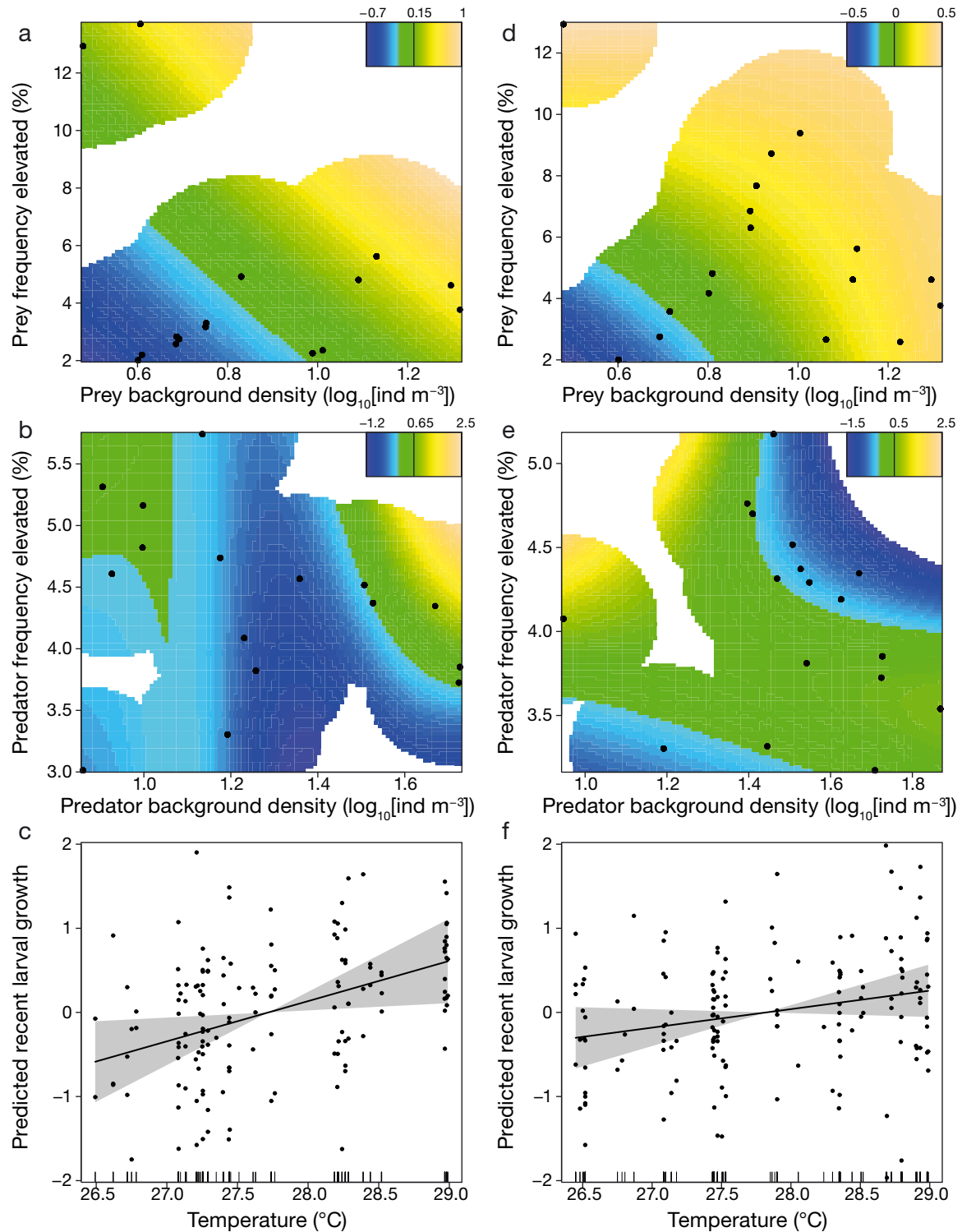|	Background density (ind. m^{-3})	Frequency elevated (%)	Elevated density minimum (ind. m^{-3})	Elevated density (ind. m^{-3})
Prey: copepods (cyclopoid & harpacticoid)	7.4 (2.0–19.7)	4.9 (2.0–13.7)	29.5 (12.9–59.6)	41.5 (14.4–192.4)
Prey: appendicularians	67.7 (30.0–111.4)	3.6 (2.3–5.3)	140.0 (79.1–207.3)	161.8 (85.3–365.7)
Predators: chaetognaths + hydromedusae	27.5 (6.2–72.9)	4.3 (3.0–5.7)	74.9 (31.4–155.9)	92.8 (32.2–335.0)

Fig. 3. Model results of (a,d) the interactive effect of prey background density (BD) and frequency elevated (FE), (b,e) the interactive effect of predator BD and FE, and (c,f) temperature on recent growth of (a–c) *Thalassoma bifasciatum* and (d–f) *Xyrichtys novacula*. Predicted recent growth is expressed as a detrended growth index and shown with warmer colors for faster growth and cooler colors for slower growth. Please note that given BD, FE, and growth values vary by prey and predator groups as well as larval fishes, both axes and scales vary among plots. For interaction plots (a,b,d,e), black dots are field observations for each interactive covariate, thus where the modeled results can best be interpreted. For temperature (c,f), fitted lines, 95 % confidence intervals (gray shaded areas) and partial residuals (dots) are shown; whiskers on *x*-axes are field observations for that covariate
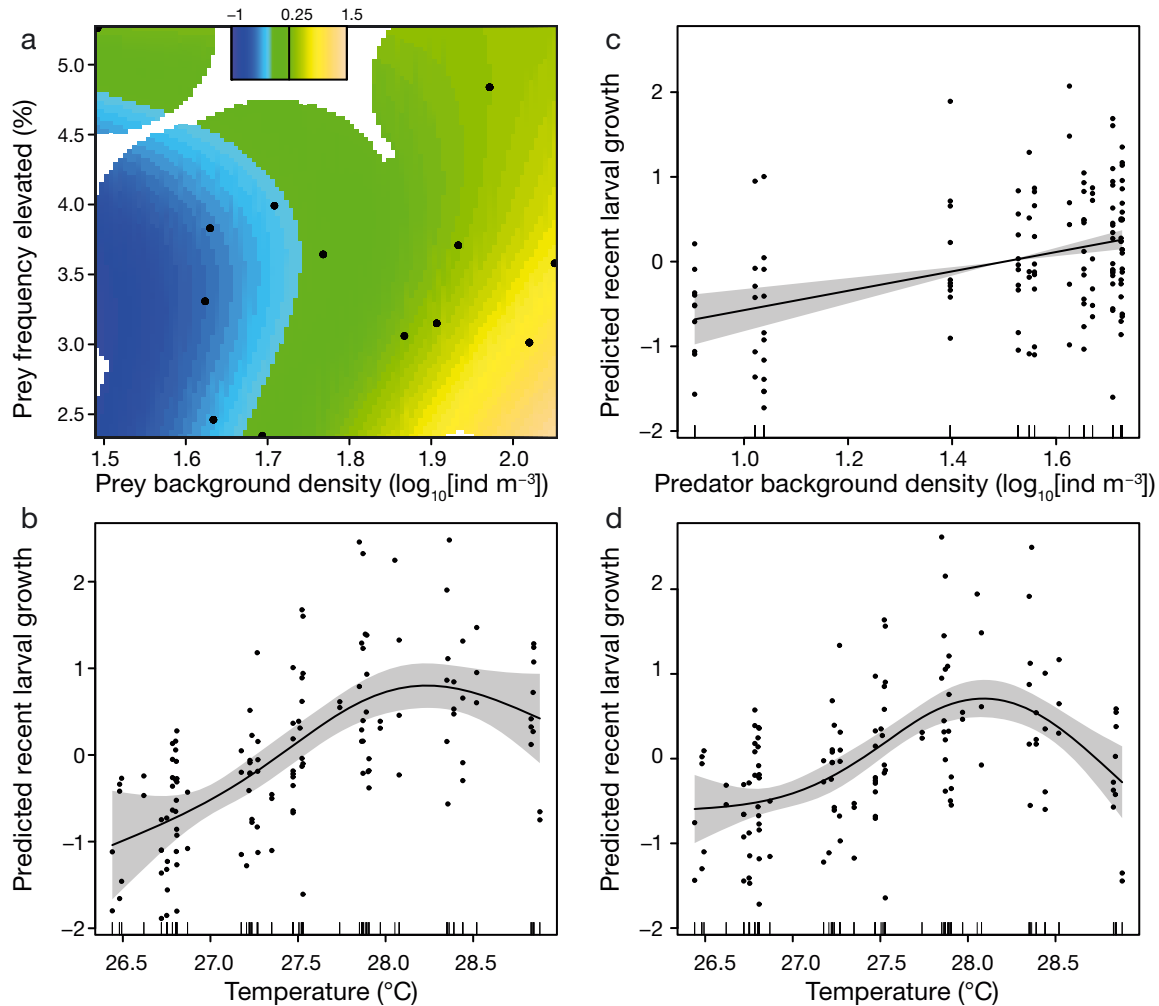
Fig. 4. Model results of (a) the interactive effect of prey background density (BD) and frequency elevated (FE), (c) predator BD, and (b,d) temperature on recent growth of *Katsuwonus pelamis*. Results are from separate (a,b) prey and (c,d) predator models. Predicted recent growth is expressed as a detrended growth index. For the prey interaction plot (a), warmer colors are faster growth, cooler colors are slower growth, and black dots are field observations for each interactive covariate, thus where the modeled results can best be interpreted. For predators and temperature (b–d), fitted lines, 95% confidence intervals (grey shaded areas) and partial residuals (dots) are shown; whiskers on *x*-axes are field observations for that covariate

and FE (Table 3, Fig. 3a). The effect of predators on recent growth was significant and bimodal, with faster growth at high (>25 ind. m^{-3}), as well as at low (<12 ind. m^{-3}) BD, but only when predators were more frequently elevated (>4%; Table 3, Fig. 3b). Recent growth was lowest at mid-range predator BD (12–25 ind. m^{-3}), regardless of the FE. There was a significant increasing relationship between recent growth and temperature (Table 3, Fig. 3c).

X. novacula had similar trends as *T. bifasciatum* in recent growth with prey (copepods) and temperature, but the relationship was non-significant for both (p < 0.1; Table 3, Fig. 3d,f). Predators significantly affected recent growth of *X. novacula*, with the lowest growth occurring when predators had both high

BD (>25 ind. m^{-3}) and FE (>4%; Table 3, Fig. 3e). Otherwise, recent growth was fairly consistent across the gradients of predator BD and FE.

For *K. pelamis*, recent growth increased significantly with prey (appendicularian) BD (Table 3, Fig. 4a). Recent growth increased slightly with prey FE at the highest range of the gradient (5%), but BD had the strongest effect on recent growth. Recent growth was strongly affected by temperature, increasing to a peak at 28°C before decreasing at higher temperatures (Table 3, Fig. 4b). The univariate predator model indicated that recent growth increased significantly with predator BD and peaked at mid-temperatures, similar to the other *K. pelamis* models (Table 3, Fig. 4c,d).

Table 3. Summary of the best generalized additive models (GAM) and interactive GAMs explaining the influence of prey and predator distributions on recent larval growth patterns of *Thalassoma bifasciatum*, *Xyrichtys novacula*, and *Katsuwonus pelamis* in the Straits of Florida. Estimated degrees of freedom (or linear coefficient in the case of parametric terms) and statistical significance are shown for each term, as well as deviance explained (Dev. exp; %), generalized cross validation (GCV), and Akaike information criterion (AIC) scores for each model. Variables are defined in Table 1 and described in Section 2. NS (not significant) denotes predictor variables removed in backward selection. Dashes denote predictor variables not included in the model. · p ≤ 0.1, *p ≤ 0.05, **p ≤ 0.01, ***p ≤ 0.001

GAMs	PreyBD	PreyFE	PredBD	PredFE	PreyBD × PreyFE	PredBD × PredFE	Depth	T	Dev. exp	GCV	AIC
T. bifasciatum	2.11***	1.00**	NS	NS	–	–	0.44**	1.00**	26.3	0.62	348.44
X. novacula	1.00***	1.11*	2.96**	2.90**	–	–	0.67**	1.98·	19.6	0.57	354.85
K. pelamis (prey)	1.00***	2.28*	–	–	–	–	NS	2.78***	32.4	0.54	300.74
K. pelamis (predator)	–	–	1.00***	–	–	–	NS	2.89***	31.3	0.55	298.66
Interactive GAMs											
T. bifasciatum	–	–	–	–	3.01***	7.26*	NS	1.00*	31.5	0.63	350.12
X. novacula	–	–	–	–	3.00·	5.89***	NS	1.00·	21.8	0.54	348.44
K. pelamis (prey)	–	–	–	–	4.19***	–	NS	2.67***	33.9	0.54	299.28

4. DISCUSSION

4.1. Prey availability and larval growth

The wrasses *Thalassoma bifasciatum* and *Xyrichtys novacula* occupy a substantially different ecological niche than skipjack tuna *Katsuwonus pelamis*. The wrasses are slower-growing (~0.25 mm d⁻¹) larvae that prey on cyclopoid and harpacticoid copepods (Sponaugle et al. 2009) and range from moderately abundant to rare and patchy. In contrast, skipjack tuna larvae are fast-growing (0.44 mm d⁻¹) and prey on highly abundant, ubiquitous appendicularians (Llopiz et al. 2010). This variability in prey selection and larval growth sets the stage for a comparison in the relationship between recent growth and prey availability.

For all 3 species, recent larval growth increased with prey background density (BD), with the fastest growth occurring on transects with the highest average prey densities. But average densities do not fully explain the effect prey has on larval fish growth. High-density patches of prey on otherwise low prey density transects can also support faster larval growth. For larvae of both wrasse species, recent growth increased with the frequency of elevated patches of prey (FE). Both wrasses had high recent growth at high prey BD (20 ind. m⁻³) but also at low BD (2 ind. m⁻³) when prey was more frequently elevated (higher FE). In fact, at low BD, prey were elevated to 21 to 82 ind. m⁻³ in 13% of the transect, indicating that dense patches of prey can be as beneficial for growth as consistently abundant prey. Yet, larvae collected from regions of low prey BD, without high

FE, did not experience the same growth advantage. In comparison to the wrasses, *K. pelamis* growth increased primarily with prey BD and less so with prey FE. This pattern reflects the natural distributions of their prey in the SOF: appendicularians are consistently highly abundant, with elevated prey densities present in only 2 to 5% of the transect.

Patchiness of plankton has been well documented (Mackas et al. 1985, Davis et al. 1991) and frequently hypothesized to be important for larval fish growth and survival, especially in regions with low prey concentrations (Houde & Schekter 1978, Pepin et al. 2014). However, logistical sampling challenges have made testing these hypotheses in the wild near impossible. Here, the coupling of fine-scale plankton sampling with fine-scale otolith growth analysis has enabled us to examine larval fish growth in the context of the fine-scale distributions of their prey. By quantifying the prey FE in 1 m horizontal bins across a transect, we estimated the probability of a larval fish encountering high densities of prey on the scale of a larval fish. Additionally, the application of a multiplicative modeling approach revealed how these high-density patches of prey can further benefit larval growth beyond relationships with average concentrations of prey.

The contrast in the relative importance of patchy prey to recent growth for the wrasses versus the tuna is consistent with experimental evidence suggesting that not all larvae may benefit from patchy prey (Houde & Schekter 1978, 1981). Additionally, recent studies examining relationships between larval feeding success and growth also suggest a difference in prey utilization between fast- and slow-growing lar-

val fishes (Dower et al. 2009, Pepin et al. 2014, Robert et al. 2014). Fast growers (i.e. scombrids) had a strong correlation between larval growth and gut contents as well as a higher degree of autocorrelation in daily growth, suggesting consistently high feeding rates and highly important early feeding success (Pepin et al. 2014). In comparison, slow growers (including *T. bifasciatum*) had weaker correlations between larval growth and gut contents, indicative of feeding on more variable or patchy prey, and potential resilience to episodes of poor feeding success (Pepin et al. 2014). In our study, variation in larval growth with prey patchiness further reinforces the existence of diverse larval strategies that include different suites of larval traits and foraging on distinctly different prey. The slow-growing wrasses and fast-growing skipjack tuna reflect two contrasting evolutionary adaptations to exploit resources in an oligotrophic planktonic food web (Llopiz 2013).

4.1.1. Slow-growing wrasses with patchy prey

T. bifasciatum and *X. novacula* in the SOF exhibit highly selective feeding for cyclopoid and harpacticoid copepods (Llopiz & Cowen 2009, Sponaugle et al. 2009), yet calanoids (2- to 8-fold more abundant; unpubl. data) are the dominant copepods in the plankton. While such specialization may reduce competition for resources, it likely increases energy expended as larvae search for prey and is thus counter to optimal foraging theories (Pyke et al. 1977). Yet, diet analyses of *T. bifasciatum* and *X. novacula* larvae in the SOF indicate survivors are successfully feeding, with almost all collected larvae having full guts (Llopiz & Cowen 2009, Sponaugle et al. 2009). Interestingly, our results suggest that larvae can successfully exploit high-density patches of prey, when present, to enhance growth. For species with relatively slow larval growth, periods of elevated growth may be sufficient to allow survival in an otherwise food-limited environment. This may be a strategy that these subtropical larvae have evolved to survive in this oligotrophic region. *T. bifasciatum* has a highly variable pelagic larval phase, with individuals within and among cohorts varying in growth, pelagic larval duration (PLD), and size-at-settlement (Searcy & Sponaugle 2000, 2001). With similar prey, growth rates, and relationships to prey availability as *T. bifasciatum*, *X. novacula* larvae have a similarly plastic early life history strategy (Hare & Cowen 1991). Previous studies have hypothesized that the slow growth rate, low daily rations, and plasticity in larval traits

for *T. bifasciatum* larvae enable them to survive in a highly variable pelagic environment with patchy prey (Sponaugle & Pinkard 2004). The increase in larval growth these species exhibit across a strong gradient of cyclopoid and harpacticoid copepod BD and FE is consistent with this hypothesis.

Larval growth has previously been shown to vary with prey abundance for coral reef fishes in the SOF, but only over broad regional scales or across mesoscale physical features. Sponaugle et al. (2009) found *T. bifasciatum* to have faster growth, larger size-at-age, and fuller guts in the more productive western SOF where prey abundances are generally higher compared to the eastern regions. Further, *T. bifasciatum* and *X. novacula* associated with productive mesoscale eddies had faster growth and larger sizes-at-age compared to larvae outside of the eddies, likely due to higher prey availability (Shulzitski et al. 2015, 2016). Our results echo these patterns but are the first to demonstrate a direct relationship between larval growth and prey availability across a gradient of prey densities and, importantly, prey patchiness. Previous studies have shown that faster larval growth not only enhances larval survival (Shulzitski et al. 2016) but also can 'carry-over' to increase the survival of juveniles (Sponaugle et al. 2006). Faster-growing *T. bifasciatum* undergo metamorphosis at younger ages (Grorud-Colvert & Sponaugle 2011) and smaller sizes, but in a higher condition (Searcy & Sponaugle 2000), and these smaller, higher-condition juveniles can swim faster to evade predators (Grorud-Colvert & Sponaugle 2006). Such growth-related traits are key to survival of early stages, and our findings point to the importance of examining larval fish traits over gradients of not only prey density but also prey patchiness, especially in larvae with slower growth and more variable larval traits.

4.1.2. Fast-growing tuna with ubiquitous prey

K. pelamis in the SOF feed almost exclusively on appendicularians prior to a rapid (at ~7 mm SL) switch to piscivory (Llopiz et al. 2010). Studies of other fast-growing fish larvae have shown that such rapid growth is not resilient to periods of poor feeding success so reliance on a consistently abundant prey is critical (Pepin et al. 2014, Robert et al. 2014). Based on growth rates measured in our study, *K. pelamis* larvae in the SOF only have 7 to 10 d to develop the predation capabilities (e.g. digestive system, eyes, and swimming abilities) to achieve piscivory. Therefore, there is a premium on their ability to efficiently

find, attack, and capture prey, without expending much additional energy (optimal foraging theory; Pyke et al. 1977). High densities of appendicularians in the SOF substantially reduce predator search time. Appendicularian feeding by larval tunas is suggested as a nutritional 'loophole' for larvae to gain sufficient resources in an oligotrophic region by exploiting energy from the microbial loop (Bakun & Broad 2003, Llopiz et al. 2010). Our results demonstrate that appendicularians are ubiquitous in the SOF, occurring in consistently high densities, likely making them a reliable prey fueling the rapid growth and development of tuna larvae.

Comparison of these data on the natural variation in growth of *K. pelamis* in relation to environmental prey densities to other studies of larval tuna growth reinforces the concept that the fast growth of *K. pelamis* is due to their efficient feeding on appendicularians. Locally in the SOF, larval tuna success has been related to appendicularian densities: both co-occur in the upper 50 m, and gut evacuation experiments with *Auxis* sp. across seasons and years revealed that the highest feeding rates were associated with the highest environmental abundance of appendicularians (Llopiz et al. 2010). Elsewhere, fast growth in yellowfin tuna larvae was associated with the highest zooplankton volumes in the Panama Bight (Wexler et al. 2007), and bullet tuna larvae grew faster in the Mediterranean Sea where prey were more abundant, compared to the Atlantic Ocean (Laíz-Carrión et al. 2010).

Fast larval growth in high prey conditions can translate to higher survival during the larval and even juvenile phases, which can have important consequences for recruitment. For Pacific bluefin tuna larvae, faster growth leads to higher survival: survivors were larger-at-age and grew faster than the initial population in studies that either tracked cohorts (Satoh et al. 2013) or compared old and young larvae (Tanaka et al. 2006). Satoh et al. (2013) additionally showed that faster growth of survivors was significantly related to prey densities and sea surface temperature. Lack of sufficient prey can lead to starvation and reduced survival in these fast-growing species (see for example, Tanaka et al. 2008), although slow-growth in Atlantic bluefin tuna can be advantageous in low prey conditions (Blanco et al. 2018). But larval tunas in the SOF, including *K. pelamis*, have some of the highest feeding incidences worldwide for tunas, with 99% of collected larvae having prey in their gut (Llopiz et al. 2010, Llopiz 2013). Prey depletion by larvae is also unlikely, since even at lower densities appendicularians in the SOF were 4000- to 22 000-fold more abundant than *K. pe-*

lamis, and appendicularian generation times in warm water are very rapid (1–2 d; Hopcroft & Roff 1995), so their populations can withstand strong predation pressure (Llopiz et al. 2010). Therefore, the slower-growing *K. pelamis* larvae in lower-density prey conditions may not experience significantly reduced feeding, but this slow growth could result in reduced survival as larvae switch to piscivory and eventually metamorphose into juveniles. The switch to piscivory in tunas is a critical period in their larval phase; faster larval growth enables an earlier switch to piscivory, and delays in the shift due to slow growth can reduce growth rates even further (Reglero et al. 2014).

4.2. Predation pressure and larval growth

The partial effect of predators on growth was important for all 3 species, and recent growth varied with both predator BD and FE. The strength and direction of the predation effect was species-specific with evidence of selective loss of both fast- and slow-growing larvae. Variability in the direction of the effect of predation on growth is not unexpected. The conventional growth-survival paradigm (GSP; Houde 1987, Anderson 1988, Cushing 1990) posits that faster-growing larvae have a higher probability of survival through larger size and reduced vulnerability to gape-limited predators (Miller et al. 1988), shorter time spent vulnerable to predation (Houde 1989), and higher growth and condition, thus enhanced predator detection abilities (Takasuka et al. 2003, 2007). But there is accumulating evidence contrary to this paradigm (Takasuka et al. 2017) and broad recognition that selective mortality patterns can vary widely and be dependent on fish species, habitat, and size and type of predators.

For *T. bifasciatum*, there was an increase in the strength of selective mortality (as measured by growth patterns) with an increase in predator density: the fastest larval growth occurred at the highest BD of predators (>25 ind. m^{-3}). This suggests selective loss of the slow-growing larvae due to strong predation pressure, evident from apparent faster growth among the survivors (Meekan & Fortier 1996). High-density patches of predators, at otherwise low BD, also have a growth-selective effect on larval *T. bifasciatum*, with growth increasing with the FE of predators. This further suggests selection against slow growers in locations (patches) where predation pressure may be elevated 2- to 44-fold higher than BD. While this is in agreement with the GSP, it contrasts prior findings in the SOF. Previous studies comparing young *T. bifasciatum* larvae in the

SOF to older survivors has suggested that larvae experience selection against fast growers (Sponaugle et al. 2011, Shulzitski et al. 2016). But these studies did not distinguish individual effects of prey and predators and either averaged multiple cohorts over broad time scales (Sponaugle et al. 2011) or sampled when water temperatures were 2°C warmer than our study, when metabolic demands may make fast growth a liability (Shulzitski et al. 2016).

Growth of *K. pelamis* also increased with the BD of predators, suggesting a greater proportion of slower-growing larvae were culled from the population in locations with high (>30 ind. m^{-3}) compared to low (<10 ind. m^{-3}) predator densities. In another scombrid, the Atlantic mackerel, strong selection predation against slow growers in some years was evident by fast larval growth of surviving larvae, and this had significant implications for annual recruitment (Robert et al. 2007). We note that prey (appendicularian) and predator BD for *K. pelamis* were collinear, and we were only able to model the partial effect of predators (and temperature) on recent growth; therefore, it is possible that the fast larval growth of *K. pelamis* is due to co-occurring high densities of predators and prey.

Most of the stations used to examine *X. novacula* growth had high predator BD (24–72 ind. m^{-3}) and among these locations, the predator FE had a stronger effect on recent larval growth than BD. Slower larval growth was associated with more frequent high-density (77–330 ind. m^{-3}) patches of predators (higher FE). This pattern suggests that predators selectively preyed upon fast growers, resulting in the preponderance of slower growers among the survivors we sampled, in contrast to the GSP and predation effect on *T. bifasciatum* and *K. pelamis*. Higher predation on faster-growing, larger larvae is thought to be due to heightened foraging activity and, consequently, higher encounter rates with predators, compared to smaller, less active larvae (Litvak & Leggett 1992, Paradis et al. 1999). Within the wrasses, *X. novacula* was larger-at-age and had a higher mean somatic growth rate (0.26 mm d^{-1}) compared to *T. bifasciatum* (0.21 mm d^{-1}). The larger size (~7 mm SL) and potentially greater swimming activity may make larger *X. novacula* more vulnerable to predation mortality than *T. bifasciatum* (~5 mm SL). *X. novacula* was also substantially larger than *K. pelamis* (~5 mm SL), which may further account for these contrasting vulnerability patterns.

Quantifying larval mortality from predation is challenging, and our study is among the first to directly relate larval fish growth to environmental predator densities and spatial distributions in any marine environment. Locally in the SOF, predation pressure on larval fishes has been predicted to be regionally strong in the more productive western SOF (Sponaugle et al. 2009, Llopiz 2013), but quantification of the distribution and abundance of predator populations has been limited by sampling technology. *In situ* imaging now enables enumeration of gelatinous zooplankton, especially those of smaller sizes (mm to cm) that can be important predators on larval fishes (Bailey & Houde 1989) but have previously been too small and fragile to properly be estimated with conventional net sampling (Luo et al. 2014). Additionally, the modeling approach we used enables the contrasting effects of prey, predators, and temperature on larval growth to be disentangled by examination of the partial effects of each component. However, a full examination of the direct impacts of predation on larval fish growth is difficult in a dynamic pelagic ecosystem due to the wide array of predator sizes, types, and other prey choices (Bailey & Houde 1989). For example, growth-selection is dependent on the size ratio of prey to predators (~10%; Paradis et al. 1999). While the predators considered in our study (chaetognaths and hydromedusae) vary in size, we assumed that the relative proportions of predator sizes are consistent across sampling locations. Additionally, we recognize that chaetognaths and hydromedusae also feed on common zooplankton in the SOF (e.g. copepods, crustacean larvae, smaller hydromedusae; Baier & Purcell 1997, Regula et al. 2009), but with the densities of predators exceeding larval fishes by 100 to 26000 times, a strong growth-selective effect by predators was present.

4.3. Temperature and larval growth

For all 3 species, temperature had a significant effect on recent larval growth. For both wrasses, growth was positively related to temperature, similar to many larval fishes (Houde 1989). This is consistent with prior studies that demonstrated a strong effect of temperature on larval growth for coral reef fishes, despite the relatively small seasonal variation in temperature in these regions (McCormick & Moloney 1995, Sponaugle et al. 2006, D'Alessandro et al. 2013). High plasticity in growth-related traits in these species suggests they may be resilient to variable environmental conditions. Hindcasted larval growth from 13 cohorts of juveniles indicated that larval growth in *T. bifasciatum* varies directly with temper-

ature, with faster-growing larvae in warmer water spending up to 15 fewer days in the plankton before settling to the reef (Sponaugle et al. 2006). Larval encounter with different water temperatures can also 'carry-over' to influence the composition of settling juveniles: in addition to being younger at settlement, *T. bifasciatum* settling in warmer temperatures were smaller and of higher condition at settlement and grew faster as juveniles, compared to fish settling during cooler water temperatures (Grorud-Colvert & Sponaugle 2011).

In contrast, the skipjack tuna *K. pelamis* had a dome-shaped relationship with growth peaking at an optimal temperature, suggesting the existence of constraints at higher temperatures. Such temperature-related growth curves are common in poikilo-thermic (cold-blooded) organisms as there is typically an optimal thermal range that controls physiological processes (Fry 1971, Jobling 1981, Takasuka et al. 2007). Further, there may also be a food-related constraint on growth at the highest temperatures. Although their appendicularian prey are plentiful in the SOF, and prior gut content analyses have revealed high gut fullness (Llopiz et al. 2010), *K. pelamis* rapidly transition to piscivory at ~7 mm (Llopiz et al. 2010) and may experience elevated energetic demands to successfully make this transition. Fast development of *K. pelamis* larvae in this study (3.4–6.6 mm) is required to prepare for piscivory (e.g. digestive tract, eyes, mouth). Larvae in the warmest temperatures may not be able to sustain these increased metabolic demands with a planktivorous diet, and if not developmentally ready to switch to piscivory, would likely experience reduced growth (and survival). This switch to piscivory is a critical period for larval Atlantic bluefin tuna in the Mediterranean Sea, and in warmer temperatures, a faster shift in diet is accompanied with higher mortality rates (Reglero et al. 2011). An earlier transition to piscivory is generally beneficial for growth and survival, and delays in this switch can result in reduced growth (Reglero et al. 2014). Compared to bluefin tuna, *K. pelamis* has a faster growth rate (Muhling et al. 2017) and more trophic specialization (Llopiz & Hobday 2015); therefore, a rapid reduction in larval growth at the highest temperatures is not surprising.

Optimal temperatures for larval tuna growth have been shown for yellowfin tuna in both the laboratory (26–31°C; Wexler et al. 2011) and natural conditions in the Gulf of Mexico (29°C; Lang et al. 1994). *K. pelamis* larvae analyzed in our study were collected in waters ranging from 26.5 to 29°C, with growth

peaking at an optimum of 28°C. Skipjack tunas generally spawn in 26 to 30°C water, and larvae have been observed in 24 to 31°C (Muhling et al. 2017, and references therein). The SOF is at the warmer end of this range (Llopiz & Hobday 2015) with temperatures up to 31°C in the warmest months (Shulzitski et al. 2016). Mortality of larval tunas can rapidly increase above optimal temperatures (Kimura et al. 2010), and larvae in marginal temperature conditions may become more vulnerable to predation due to decreases in swimming, escape, and foraging ability (Blaxter 1991). If *K. pelamis* larvae experience reduced growth above ~28°C, it appears that the warmest conditions they currently experience in the SOF are at their edge of their thermal limits.

Future warming is predicted to increase sea surface temperatures in the SOF by 3 to 4°C over the next century (Alexander et al. 2018). This will impact subtropical marine environments through enhanced thermal stratification; reducing productivity in an already oligotrophic environment (Brown et al. 2010). While the appendicularian prey of tunas are specialized to feed in this environment and benefit from these conditions (Landry et al. 2019), warming ocean temperatures are expected to increase mortality in subtropical larval fishes (Llopiz et al. 2014). Based on the optimal temperature for *K. pelamis* growth, we hypothesize that predicted warming will be detrimental to their larval growth and development needed for a shift to piscivory. These growth and survival implications should be included in future population models of this commercially important species (Lehodey et al. 2013). While the wrasses appear to be more resilient to temperature variability than the thermally constrained tunas, *T. bifasciatum* larvae previously collected in the SOF during higher temperatures (29–31°C) experienced selective loss of fast growers (compared to no evidence of selective mortality at lower temperatures of 26–28°C); Shulzitski et al. 2016). This difference was hypothesized to be due to prey conditions that could not support the high metabolic demands of fast-growing larvae in the hot conditions; lower selective loss was evident for larvae collected simultaneously from prey-rich recirculating eddies. While future changes for the copepod prey of the wrasses are unclear (Landry et al. 2019), decreased abundance or availability of high-density patches of prey could significantly constrain their larval growth. If this is compounded with warmer temperatures that increase growth rates, prey availability for the wrasses may not be enough to meet energetic demands.

5. CONCLUSIONS

The integration of fine-scale *in situ* imaging and biological samples of larval fishes demonstrated that fine-scale variability in prey and predator concentrations has important implications for larval growth. For slow-growing species such as wrasses, prey patchiness can be as important as average prey density in determining larval growth. While larvae of both wrasse species are well-adapted to feed on a rare and patchy copepod prey, their growth is constrained at low average prey densities if high-density prey patches do not occur sufficiently frequently. In contrast, fast-growing species such as skipjack tuna rely on consistently abundant prey such as appendicularians and are less dependent on prey patchiness. The distribution of predators also influences the composition of larval fish survivors, with the contrasting patterns of growth-selective predation likely related to larval fish size: selection against fast growers for the larger *Xyrichtys novacula* and selection against slow growers for the smaller *Thalassoma bifasciatum* and *Katsuwonus pelamis*. Interestingly, the strength of growth-selective predation on the wrasses increased with the frequency of high-density patches of predators. Higher temperatures promoted growth for all larvae, but an optimal growth temperature for *K. pelamis* suggests that there may be metabolic constraints at high temperatures. Early onset of piscivory in this species places a premium on fast growth and development that may be hard to sustain at the highest temperatures. The balance between water temperatures and food availability is likely to play an increasingly important role in determining the survival of larval fishes under future climate change scenarios.

LITERATURE CITED

Alexander MA, Scott JD, Friedland KD, Mills KE, Nye JA, Pershing AJ, Thomas AC (2018) Projected sea surface temperatures over the 21st century: changes in the mean, variability and extremes for large marine ecosystem regions of Northern Oceans. Elem Sci Anth 6:9

Anderson JT (1988) A review of size dependent survival during pre-recruit stages of fishes in relation to recruitment. J Northwest Atl Fish Sci 8:55−66

Baier CT, Purcell JE (1997) Effects of sampling and preservation on apparent feeding by chaetognaths. Mar Ecol Prog Ser 146:37−42

Bailey KM, Houde ED (1989) Predation on eggs and larvae of marine fishes and the recruitment problem. Adv Mar Biol 25:1−83

Bakun A, Broad K (2003) Environmental 'loopholes' and fish population dynamics: comparative pattern recognition with focus on El Niño effects in the Pacific. Fish Oceanogr 12:458−473

Baumann H, Pepin P, Davidson FJM, Mowbray F, Schnack D, Dower JF (2003) Reconstruction of environmental histories to investigate patterns of larval radiated shanny (*Ulvaria subbifurcata*) growth and selective survival in a large bay of Newfoundland. ICES J Mar Sci 60:243−258

Bils F, Moyano M, Aberle N, Hufnagl M, Alvarez-Fernandez S, Peck MA (2017) Exploring the microzooplankton–ichthyoplankton link: a combined field and modeling study of Atlantic herring (*Clupea harengus*) in the Irish sea. J Plankton Res 39:147−163

Blanco E, Reglero P, Ortega A, de la Gándara F, Folkvord A (2018) Size-selective mortality of laboratory-reared Atlantic bluefin tuna larvae: evidence from microstructure analysis of otoliths during the piscivorous phase. J Exp Mar Biol Ecol 509:36−43

Blaxter JHS (1991) The effect of temperature on larval fishes. Neth J Zool 42:336−357

Brown CJ, Fulton EA, Hobday AJ, Matear RJ and others (2010) Effects of climate-driven primary production change on marine food webs: implications for fisheries and conservation. Glob Change Biol 16:1194−1212

Castonguay M, Plourde S, Robert D, Runge JA, Fortier L (2008) Copepod production drives recruitment in a marine fish. Can J Fish Aquat Sci 65:1528−1531

Clemmesen C (1994) The effect of food availability, age or size on the RNA/DNA ratio of individually measured herring larvae: laboratory calibration. Mar Biol 118:377−382

Cowen RK, Guigand CM (2008) *In situ* ichthyoplankton imaging system (*IS*IIS): system design and preliminary results. Limnol Oceanogr Methods 6:126−132

Cushing DH (1990) Plankton production and year-class strength in fish populations: an update of the match/mismatch hypothesis. Adv Mar Biol 26:249−293

D'Alessandro EK, Sponaugle S, Cowen RK (2013) Selective mortality during the larval and juvenile stages of snappers (Lutjanidae) and great barracuda *Sphyraena barracuda.* Mar Ecol Prog Ser 474:227−242

Davis CS, Flierl GR, Wiebe PH, Franks PJS (1991) Micro-patchiness, turbulence and recruitment in plankton. J Mar Res 49:109–151

Dower JF, Pepin P, Kim GC (2009) Covariation in feeding success, size-at-age and growth in larval radiated shanny (*Ulvaria subbifurcata*): insights based on individuals. J Plankton Res 31:235–247

Fry FEJ (1971) The effect of environmental factors on the physiology of fish. In: Hoar WS, Randall DJ (eds) Fish physiology, Vol 6. Academic Press, New York, NY, p 1–98

Graham B (2014) Fractional max-pooling. arXiv:1412.6071

Greer AT, Woodson CB (2016) Application of a predator–prey overlap metric to determine the impact of sub-grid scale feeding dynamics on ecosystem productivity. ICES J Mar Sci 73:1051–1061

Greer AT, Cowen RK, Guigand CM, McManus MA, Sevadjian JC, Timmerman AHV (2013) Relationships between phytoplankton thin layers and the fine-scale vertical distributions of two trophic levels of zooplankton. J Plankton Res 35:939–956

Greer AT, Woodson CB, Smith CE, Guigand CM, Cowen RK (2016) Examining mesozooplankton patch structure and its implications for trophic interactions in the northern Gulf of Mexico. J Plankton Res 38:1115–1134

Grorud-Colvert K, Sponaugle S (2006) Influence of condition on behavior and survival potential of a newly settled coral reef fish, the bluehead wrasse *Thalassoma bifasciatum.* Mar Ecol Prog Ser 327:279–288

Grorud-Colvert K, Sponaugle S (2011) Variability in water temperature affects trait-mediated survival of a newly settled coral reef fish. Oecologia 165:675–686

Hamilton SL (2008) Larval history influences post-metamorphic condition in a coral-reef fish. Oecologia 158:449–461

Hare JA, Cowen RK (1991) Expatriation of *Xyrichtys novacula* (Pisces: Labridae) larvae: evidence of rapid cross-slope exchange. J Mar Res 49:801–823

Hare JA, Cowen RK (1997) Size, growth, development, and survival of the planktonic larvae of *Pomatomus saltatrix* (Pices: Pomatomidae). Ecology 78:2415–2431

Hitchcock GL, Lee TN, Ortner PB, Cummings S, Kelble C, Williams E (2005) Property fields in a Tortugas Eddy in the southern straits of Florida. Deep Sea Res I 52:2195–2213

Hjort J (1914) Fluctuations in the great fisheries of northern Europe viewed in the light of biological research. Rapp P-V Reun Cons Int Explor Mer 20:1–228

Hopcroft RR, Roff JC (1995) Zooplankton growth rates: extraordinary production by the larvacean *Oikopleura dioica* in tropical waters. J Plankton Res 17:205–220

Houde ED (1987) Fish early life dynamics and recruitment variability. Am Fish Soc Symp 2:17–29

Houde ED (1989) Comparative growth, mortality, and energetics of marine fish larvae: temperature and implied latitudinal effects. Fish Bull 87:471–495

Houde ED, Schekter RC (1978) Simulated food patches and survival of larval bay anchovy, *Anchoa mitchilli*, and sea bream, *Archosargus thomboidalis.* Fish Bull (Wash DC) 76:483–487

Houde ED, Schekter RC (1981) Growth rates, rations and cohort consumption of marine fish larvae in relation to prey concentrations. Rapp P-V Reun Cons Int Explor Mer 178:441–453

Jobling M (1981) Temperature tolerance and the final preferendum—rapid methods for the assessment of optimum growth temperatures. J Fish Biol 19:439–455

Kimura S, Kato Y, Kitagawa T, Yamaoka N (2010) Impacts of environmental variability and global warming scenario on Pacific bluefin tuna (*Thunnus orientalis*) spawning grounds and recruitment habitat. Prog Oceanogr 86:39–44

Laíz-Carrión R, Pérez-Torres A, Quintanilla J, García A, Alemany F (2010) Variable growth of bullet tuna larvae (*Auxis rochei*) related to hydrographic scenarios off the Balearic sea. Rapp Comm Int Mer Medit 39:563

Landry MR, Beckley LE, Muhling BA (2019) Climate sensitivities and uncertainties in food-web pathways supporting larval bluefin tuna in subtropical oligotrophic oceans. ICES J Mar Sci 76:359–369

Lang KL, Grimes CB, Shaw RF (1994) Variations in the age and growth of yellowfin tuna larvae, *Thunnus albacares*, collected about the Mississippi River plume. Environ Biol Fishes 39:259–270

Lasker R (1975) Field criteria for survival of anchovy larvae: the relation between inshore chlorophyll maximum layers and successful first feeding. Fish Bull 73:453–462

Lee TN, Yoder JA, Atkinson LP (1991) Gulf Stream frontal eddy influence on productivity of the southeast U.S. continental shelf. J Geophys Res 96:22191–22205

Lehodey P, Senina I, Calmettes B, Hampton J, Nicol S (2013) Modelling the impact of climate change on Pacific skipjack tuna population and fisheries. Clim Change 119:95–109

Litvak MK, Leggett WC (1992) Age and size-selective predation on larval fishes: the bigger-is-better hypothesis revisited. Mar Ecol Prog Ser 81:13–24

Llopiz JK (2013) Latitudinal and taxonomic patterns in the feeding ecologies of fish larvae: a literature synthesis. J Mar Syst 109–110:69–77

Llopiz JK, Cowen RK (2009) Variability in the trophic role of coral reef fish larvae in the oceanic plankton. Mar Ecol Prog Ser 381:259–272

Llopiz JK, Hobday AJ (2015) A global comparative analysis of the feeding dynamics and environmental conditions of larval tunas, mackerels, and billfishes. Deep Sea Res II 113:113–124

Llopiz JK, Richardson DE, Shiroza A, Smith SL, Cowen RK (2010) Distinctions in the diets and distributions of larval tunas and the important role of appendicularians. Limnol Oceanogr 55:983–996

Llopiz JK, Cowen RK, Hauff MJ, Ji R and others (2014) Early life history and fisheries oceanography: new questions in a changing world. Oceanography (Wash DC) 27:26–41

Luo JY, Grassian B, Tang D, Irisson JO and others (2014) Environmental drivers of the fine-scale distribution of a gelatinous zooplankton community across a mesoscale front. Mar Ecol Prog Ser 510:129–149

Luo JY, Irisson JO, Graham B, Guigand C, Sarafraz A, Mader C, Cowen RK (2018) Automated plankton image analysis using convolutional neural networks. Limnol Oceanogr Methods 16:814–827

Mackas DL, Denman KL, Abbott MR (1985) Plankton patchiness: biology in the physical vernacular. Bull Mar Sci 37:652–674

Mackenzie BR, Leggett WC, Peters RH (1990) Estimating larval fish ingestion rates: Can laboratory derived values be reliably extrapolated to the wild? Mar Ecol Prog Ser 67:209–225

McCormick MI, Moloney BW (1995) Influence of water temperature during the larval stage on size, age and body condition of a tropical reef fish at settlement. Mar Ecol Prog Ser 118:59–68

Meekan MG, Fortier L (1996) Selection for fast growth during the larval life of Atlantic cod *Gadus morhua* on the Scotian shelf. Mar Ecol Prog Ser 137:25–37

Miller TJ, Crowder LB, Rice JA, Marschall EA (1988) Larval size and recruitment mechanisms in fishes: toward a conceptual framework. Can J Fish Aquat Sci 45:1657–1670

Muhling BA, Lamkin JT, Alemany F, García A and others (2017) Reproduction and larval biology in tunas, and the importance of restricted area spawning grounds. Rev Fish Biol Fish 27:697–732

Nakata H, Kimura S, Okazaki Y, Kasai A (2000) Implications of meso-scale eddies caused by frontal disturbances of the Kuroshio Current for anchovy recruitment. ICES J Mar Sci 57:143–152

Owen RW (1989) Microscale and finescale variations of small plankton in coastal and pelagic environments. J Mar Res 47:197–240

Pannella G (1971) Fish otoliths: daily growth layers and periodical patterns. Science 173:1124–1127

Paradis AR, Pépin M, Pepin P (1999) Disentangling the effects of size-dependent encounter and susceptibility to predation with an individual-based model for fish larvae. Can J Fish Aquat Sci 56:1562–1575

Pepin P (2004) Early life history studies of prey–predator interactions: quantifying the stochastic individual responses to environmental variability. Can J Fish Aquat Sci 61:659–671

Pepin P, Robert D, Bouchard C, Dower JF and others (2014) Once upon a larva: revisiting the relationship between feeding success and growth in fish larvae. ICES J Mar Sci 72:359–373

Purcell JE, Arai MN (2001) Interactions of pelagic cnidarians and ctenophores with fish: a review. Hydrobiologia 451: 27–44

Pyke GH, Pulliam HR, Charnov EL (1977) Optimal foraging: a selective review of theory and tests. Q Rev Biol 52: 137–154

R Core Team (2019) R: a language and environment for statistical computing. R Foundation for Statistical Computing, Vienna. www.r-project.org

Radtke RL (1983) Otolith formation and increment deposition in laboratory reared skipjack tuna, *Euthynnus pelamis*, larvae. In: Proc Int Workshop on Age Determination of Oceanic Pelagic Fishes: Tunas, Billfishes, and Sharks. Feb 15–18, 1982, Miami, FL, p 99–103

Reglero P, Urtizberea A, Torres AP, Alemany F, Fiksen Ø (2011) Cannibalism among size classes of larvae may be a substantial mortality component in tuna. Mar Ecol Prog Ser 433:205–219

Reglero P, Ortega A, Blanco E, Fiksen Ø and others (2014) Size-related differences in growth and survival in piscivorous fish larvae fed different prey types. Aquaculture 433:94–101

Regula C, Colin SP, Costello JH, Kordula H (2009) Prey selection mechanism of ambush-foraging hydromedusae. Mar Ecol Prog Ser 374:135–144

Richards W (2005) Early stages of Atlantic fishes: an identification guide for the Western Central North Atlantic. CRS Press, Boca Raton, FL

Richardson DE, Llopiz JK, Leaman KD, Vertes PS, Muller-Karger FE, Cowen RK (2009) Sailfish (*Istiophorus platypterus*) spawning and larval environment in a Florida Current frontal eddy. Prog Oceanogr 82:252–264

Richardson DE, Llopiz JK, Guigand CM, Cowen RK (2010) Larval assemblages of large and medium-sized pelagic species in the Straits of Florida. Prog Oceanogr 86:8–20

Ringuette M, Fortier L, Fortier M, Runge JA and others (2002) Advanced recruitment and accelerated population development in Arctic calanoid copepods of the North Water. Deep Sea Res II 49:5081–5099

Robert D, Castonguay M, Fortier L (2007) Early growth and recruitment in Atlantic mackerel *Scomber scombrus*: discriminating the effects of fast growth and selection for fast growth. Mar Ecol Prog Ser 337:209–219

Robert D, Pepin P, Dower JF, Fortier L (2014) Individual growth history of larval Atlantic mackerel is reflected in daily condition indices. ICES J Mar Sci 71:1001–1009

Rothschild BJ, Osborn TR (1988) Small-scale turbulence and plankton contact rates. J Plankton Res 10:465–474

Satoh K, Tanaka Y, Masujima M, Okazaki M, Kato Y, Shono H, Suzuki K (2013) Relationship between the growth and survival of larval Pacific bluefin tuna, *Thunnus orientalis*. Mar Biol 160:691–702

Schmid MS, Cowen RK, Robinson K, Luo JY, Briseño-Avena C, Sponaugle S (2020) Prey and predator overlap at the edge of a mesoscale eddy: fine-scale, in-situ distributions to inform our understanding of oceanographic processes. Sci Rep 10:921

Searcy SP, Sponaugle S (2000) Variable larval growth in a coral reef fish. Mar Ecol Prog Ser 206:213–226

Searcy SP, Sponaugle S (2001) Selective mortality during the larval-juvenile transition in two coral reef fishes. Ecology 82:2452–2470

Shulzitski K, Sponaugle S, Hauff M, Walter K, Alessandro EK, Cowen RK (2015) Close encounters with eddies: oceanographic features increase growth of larval reef fishes during their journey to the reef. Biol Lett 11: 20140746

Shulzitski K, Sponaugle S, Hauff M, Walter KD, Cowen RK (2016) Encounter with mesoscale eddies enhances survival to settlement in larval coral reef fishes. Proc Natl Acad Sci USA 113:6928–6933

Shulzitski K, Sponaugle S, Hauff M, Walter KD, D'Alessandro EK, Cowen RK (2018) Patterns in larval reef fish distributions and assemblages, with implications for local retention in mesoscale eddies. Can J Fish Aquat Sci 75: 180–192

Sponaugle S (2009) Daily otolith increments in the early stages of tropical fish. In: Green BS, Mapstone BD, Carlos G, Begg GA (eds) Tropical fish otoliths: information for assessment, management and ecology. Springer Netherlands, Dordrecht, p 93–132

Sponaugle S, Pinkard DR (2004) Impact of variable pelagic environments on natural larval growth and recruitment of the reef fish *Thalassoma bifasciatum*. J Fish Biol 64:34–54

Sponaugle S, Grorud-Colvert K, Pinkard D (2006) Temperature-mediated variation in early life history traits and recruitment success of the coral reef fish *Thalassoma bifasciatum* in the Florida Keys. Mar Ecol Prog Ser 308: 1–15

Sponaugle S, Llopiz JK, Havel LN, Rankin TL (2009) Spatial variation in larval growth and gut fullness in a coral reef fish. Mar Ecol Prog Ser 383:239–249

Sponaugle S, Walter KD, Denit KL, Llopiz JK, Cowen RK (2010) Variation in pelagic larval growth of Atlantic billfishes: the role of prey composition and selective mortality. Mar Biol 157:839–849

Sponaugle S, Boulay JN, Rankin TL (2011) Growth- and size-selective mortality in pelagic larvae of a common reef fish. Aquat Biol 13:263–273

Takasuka A, Aoki I, Mitani I (2003) Evidence of growth-selective predation on larval Japanese anchovy *Engraulis japonicus* in Sagami Bay. Mar Ecol Prog Ser 252:223–238

Takasuka A, Oozeki Y, Aoki I (2007) Optimal growth temperature hypothesis: Why do anchovy flourish and sardine collapse or vice versa under the same ocean regime? Can J Fish Aquat Sci 64:768–776

Takasuka A, Sakai A, Aoki I (2017) Dynamics of growth-based survival mechanisms in Japanese anchovy (*Engraulis japonicus*) larvae. Can J Fish Aquat Sci 74:812–823

Tanabe T, Kayama S, Ogura M, Tanaka S (2003) Daily increment formation in otoliths of juvenile skipjack tuna *Katsuwonus pelamis.* Fish Sci 69:731–737

Tanaka Y, Satoh K, Iwahashi M, Yamada H (2006) Growth-dependent recruitment of Pacific bluefin tuna *Thunnus orientalis* in the northwestern Pacific Ocean. Mar Ecol Prog Ser 319:225–235

Tanaka Y, Satoh K, Yamada H, Takebe T, Nikaido H, Shiozawa S (2008) Assessment of the nutritional status of field-caught larval Pacific bluefin tuna by RNA/DNA ratio based on a starvation experiment of hatchery-reared fish. J Exp Mar Biol Ecol 354:56–64

Victor BC (1982) Daily otolith increments and recruitment in two coral-reef wrasses, *Thalassoma bifasciatum* and *Halichoeres bivittatus.* Mar Biol 71:203–208

Wexler JB, Chow S, Wakabayashi T, Nohara K, Margulies D (2007) Temporal variation in growth of yellowfin tuna (*Thunnus albacares*) larvae in the Panama Bight, 1990–97. Fish Bull 105:1–18

Wexler JB, Margulies D, Scholey VP (2011) Temperature and dissolved oxygen requirements for survival of yellowfin tuna, *Thunnus albacares*, larvae. J Exp Mar Biol Ecol 404:63–72

Wood SN (2006) Generalized additive models: an introduction with R. Chapman and Hall/CRC Press, Boca Raton, FL

Young KV, Dower JF, Pepin P (2009) A hierarchical analysis of the spatial distribution of larval fish prey. J Plankton Res 31:687–700